

AUTOMATIC SPACE RESECTION USING A CONSTRAINED RELATIONAL MATCHING

Aluir Porfírio Dal Poz*

Antonio Maria Garcia Tommaselli*

*Sao Paulo State University - Pres. Prudente, SP - Brazil

Department of Cartography

{aluir, tomaseli}@prudente.unesp.br

Working Group III/1

KEY WORDS: Digital Photogrammetry, Straight Lines, Automation, Relational Matching, IEKF.

ABSTRACT

Image orientation is a basic problem in Digital Photogrammetry. While interior and relative orientations have been successfully automated, the absolute orientation (or space resection) continues to be an important topic for research. An approach has been developed to automate the absolute orientation based on relational matching and a heuristic that uses the analytical relation between image and object-space straight lines. A build-in self-diagnosis is also integrated in this method, involving the implementation of data snooping statistic test in the process of spatial resection using the Iterated Extended Kalman Filtering (IEKF). The aim of this paper is to present the basic principles of the proposed approach and results based on real data.

1 INTRODUCTION

Considerable progresses have been accomplished in the automation of several geometric tasks, as, for example, the interior and relative orientation and the generation of digital orthophoto. However, the situation is quite different for semantic tasks, like the linear feature extraction from digital images for GIS data capture and updating and absolute orientation. Concerning this last one, the main difficulty is related to the fact that a correspondence process needs to be performed between a digital image and a symbolic model describing the ground control. In such a case, line-based methods are potentially better, because lines are easier to be detected in digital images and grouped than points.

In this paper, we are interested in a special class of lines, i.e., the straight lines. A simpler photogrammetric model can be derived for this type of entity, whose complexity is similar to the well-known collinearity equation. Some straight line-based photogrammetric models have been developed and can be found, for example, in Tommaselli and Lugnani (1988), Mulawa and Mikhail (1988), Tommaselli and Tozzi (1996), and Tommaselli and Dal Poz (1999).

Although linear features are easier to locate than points and can be determined with sub-pixel precision, the automatic feature extraction and correspondence is a difficult task to solve properly. A combination of several approaches is proposed in this paper. Image orientation is recursively improved using IEKF (Iterative Extended Kalman Filtering) and the feature extraction process is constrained by the filter feedback. This process was firstly applied in Machine Vision (Tommaselli and Tozzi, 1996) but the feature extraction and the matching methods were not suitable to aerial images. Since then, a relational matching method has been developed (Dal Poz et al, 1996; Dal Poz and Tommaselli, 1998) and feature extraction algorithm has been improved as well (Tommaselli and Dal Poz, 1999).

The proposed solution is described in the section 2. The results based on real data are presented and discussed in the section 3. Finally, conclusions are given in the section 4.

2 THE PROPOSED SOLUTION

The basic input data are the digital image, the ground control groupings (A_1, \dots, A_n), and the interior and approximate exterior orientation parameters. Ground control groupings correspond to local structures (e.g., road crossing) and can be extracted by measuring two 3D endpoints by conventional field survey or by photogrammetric plotting. The automatic orientation process is carried out in three main steps. First, a ground control grouping is selected (e.g., A_i) and its position in the image-space is predicted and the feature extraction process is applied only to a small window enclosing

the predicted grouping (a_i), instead of on the whole image. Second, the relational descriptions for straight lines of homologous grouping (a_i and a'_i) are accomplished. Finally, the matching strategy is applied to identify the correct correspondences between straight lines of grouping a_i and a'_i . This strategy is then repeated for other homologous groupings.

2.1 Feature Extraction

The feature extraction is applied only in the small window enclosing the predicted position of the selected ground control grouping. The following steps are then sequentially applied to the automatically extracted sub-image: 1- gradient magnitude and direction are computed for each pixel; 2- an automatic thresholding process eliminates those pixels with low gradient response; 3- edges are thinned with non-maxima suppression; 4- isolated pixel are eliminated; 5- edge pixels are labeled and connected; and 6- a line fitting is finally applied to compute the straight line parameters and the endpoints of each segmented line. Details of this method can be found in Tommaselli and Dal Poz (1999).

The results of this step are the predicted grouping (a_i) and the extracted grouping (a'_i). The prediction process is initially carried out by using the approximate exterior orientation parameters ($k, \bar{t}, w, X_o, Y_o, Z_o$) and those filtered by IEKF after each correspondence is obtained. The related covariance matrixes are used to define the window where the grouping a'_i is to be extracted.

2.2 Relational Descriptions for Homologous Groupings

The relational descriptions are established for each straight line of homologous groupings (a_i and a'_i). A relational description is a list of relations. Let O_A be an object and A be the set of its parts. An N-ary relation over A is a subset of the Cartesian product $A^N = A \times \dots \times A$ (N times) (Shapiro and Haralick, 1987).

A special type of relation, called star structure, is used in the matching strategy. As defined by Cheng and Huang (1984), a star structure rooted at node i is node i itself plus all its links and neighboring nodes. Let consider the straight lines $f_i \in a'_i$ and $f_r \in a_i$. Thus, the following relational descriptions based on star structure, whose roots are f_i and f_r (figure 1), can be written:

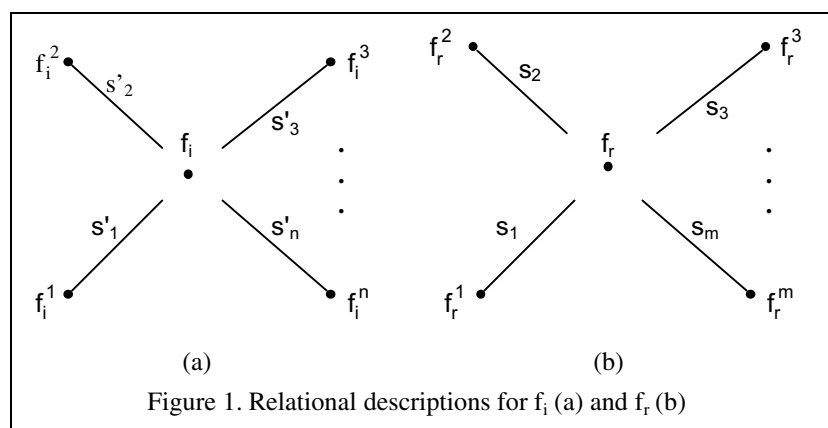


Figure 1. Relational descriptions for f_i (a) and f_r (b)

$$S_{a'_i}^{f_i} = \{S'\} = \{s'_j\}_{j=1, \dots, n} = \{s'_1, \dots, s'_n\} \tag{1}$$

$$S_{a_i}^{f_r} = \{S\} = \{s_k\}_{k=1, \dots, m} = \{s_1, \dots, s_m\} \tag{2}$$

In the figure 1(a), n is the number of neighboring nodes in the star $S_{a'_i}^{f_i}$ and f_i is its root node. The neighboring nodes are the straight lines f_i^1, \dots, f_i^n . Therefore, the $n+1$ nodes in the star $S_{a'_i}^{f_i}$ are the straight lines of grouping a'_i . Similarly, the figure 1(b) shows the star $S_{a_i}^{f_r}$, whose components are the m straight lines f_r^1, \dots, f_r^m (i. e., the neighboring nodes) and the straight line f_r , i. e., the root node.

Each component (or links) of the star structure $S_{a'_i}^{f_i}$ (or $S_{a_i}^{f_r}$) is a 5-tuple, expressed generically as follows:

$$s = (f_1, f_2, a_1, a_2, a_3) \tag{3}$$

where (figure 2),

- f_1 and f_2 are two straight lines of a star;
- a_1 is the angle between straight lines f_1 and f_2 ;
- a_2 is the angle between the bisector of f_1 and f_2 and the axis ox ; and
- a_3 is the distance between the origin of the photographic reference system (oxy) and the intersection of straight lines f_1 and f_2 , or their extensions.

The attribute a_3 is unstable whenever the straight lines f_1 and f_2 are close to parallel. In this case, the attribute a_3 is taken as the distance between the two straight lines.

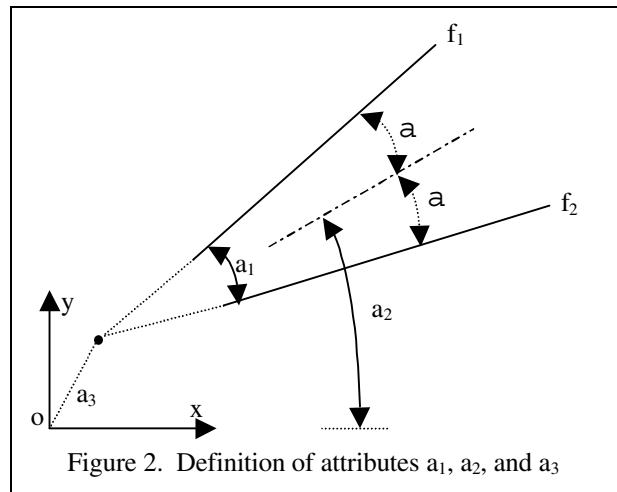


Figure 2. Definition of attributes a_1 , a_2 , and a_3

2.3 Matching Strategy

Three different criteria are applied sequentially in the matching process to check the correspondence between a straight line (f_i) from the grouping a_i and another (f_i) from the grouping a'_i . First, the so-called rigidity constraint is used as a first filter for the correspondence that is being analyzed (f_i, f_r). Next, this correspondence is checked by the relational distance (nrd). Finally, a statistical decision based on data snooping test is used for verifying whether the correspondence (f_i, f_r) is accepted or not.

2.3.1 Rigidity Constraint. As explained previously, the homologous groupings a'_i and a_i are obtained by using, respectively, a feature extraction method and the camera model. The differences in position between the two groupings are explained by considering the errors in both processes, i.e., the feature extraction and the projection of the object-space grouping (A_i).

The better the exterior orientation parameters are, the smaller is the deformation of grouping a_i . Since the exterior orientation parameters are refined by IEKF whenever a successful correspondence is obtained, that deformation is then reduced accordingly.

From the above argument, the knowledge of deformation of grouping a_i makes possible to know whether the correspondence (f_i, f_r) is possible or not. In practice, the rigidity constraint criterion is carried out by generating a search window around the straight line f_r , whose dimensions depend on the uncertainty of the camera parameters. If the straight line f_i belongs to this window, the correspondence (f_i, f_r) is considered compatible and the next criterion must be applied.

2.3.2 Relational Distance. Let $S_{a_i}^{f_i} = \{S'\}$ and $S_{a_i}^{f_r} = \{S\}$ be relational descriptions for straight lines f_i and f_r , represented respectively by equations 1 and 2, and h a function that maps primitives from star S' to star S . An expression can be written for total error $E(h)$ between $S_{a_i}^{f_i}$ and $S_{a_i}^{f_r}$ (Shapiro and Haralick, 1987):

$$E(h) = |S' \circ h - S| + |S \circ h^{-1} - S'| \tag{4}$$

where, $| \cdot |$ means cardinality. Thus, $|S' \circ h - S|$ represents the number of relations that are not mapped by h from star S' to star S and $|S \circ h^{-1} - S'|$ represents the number of relations that are not mapped by h^{-1} (inverse of h) from star S to star S' . Therefore, $E(h)$ is the total number of relations that are not mapped by h and its inverse (h^{-1}). If $E(h)=0$, h is called a relational isomorphism and S and S' are said to be isomorphic. In such a case, f_i and f_r are said to be compatible.

Now, an expression can be written representing the relational distance between relational descriptions $S_{a_i}^{f_i}$ and $S_{a_i}^{f_r}$:

$$RD(S_{a_i}^{f_i}, S_{a_i}^{f_r}) = \text{minimum}(E(h)) \tag{5}$$

The relational distance can be normalized in the range [0; 1], as follows:

$$RDN(S_{a_i}^{f_i}, S_{a_i}^{f_r}) = RD(S_{a_i}^{f_i}, S_{a_i}^{f_r}) / NC \tag{6}$$

where, NC is the total number of components in the stars S' and S.

In an ideal condition, the correspondence (f_i, f_r) is compatible when RDN(S_{a_i}^{f_i}, S_{a_i}^{f_r})= 0, and the opposite when RDN(S_{a_i}^{f_i}, S_{a_i}^{f_r})= 1. However, in practical applications, it will be necessary to use a threshold (0<L<1). The correspondence (f_i, f_r) is compatible when RDN(S_{a_i}^{f_i}, S_{a_i}^{f_r})<L.

2.3.3 Self-diagnosis. The self-diagnosis is the last criterion to be evaluated in order to verify whether the correspondence (f_i, f_r (or F_r)) that is being analyzed is accepted or not. In opposition to the two previous criterion, the self-diagnosis is a statistical decision. It is only applied if the two previous criteria are satisfied. At this step the state vector is also filtered using the observed parameters of the straight lines.

Self-diagnosis is based on the data snooping statistical test implemented with the process of space resection using the IEKF. The photogrammetric model (Tommaselli and Tozzi, 1996) is based on the geometry that is shown in figure 3.

The geometry of the figure 3 is modeled by the following equation:

$$a = - \frac{r_{11} \cdot nx + r_{12} \cdot ny + r_{13} \cdot nz}{r_{21} \cdot nx + r_{22} \cdot ny + r_{23} \cdot nz} \tag{7}$$

$$b = - f \cdot \frac{r_{31} \cdot nx + r_{32} \cdot ny + r_{33} \cdot nz}{r_{21} \cdot nx + r_{22} \cdot ny + r_{23} \cdot nz}$$

where,

- n_x= -n.(Y_o - Y₁) + m.(Z_o - Z₁);
- n_y= n.(X_o - X₁) + l.(Z_o - Z₁);
- n_z= -m.(X_o - X₁) + l.(Y_o - Y₁);
- X_o, Y_o, Z_o are the object-space coordinates of the perspective center (PC) of the camera;
- X₁, Y₁, Z₁ are the object-space coordinates of a known point on the object straight line;
- l, m, n are the components of the direction vector \vec{d} of the object-space straight line;
- r_{ij}, 1 ≤ i ≤ 3 and 1 ≤ j ≤ 3, are the elements of a rotation matrix, defined by the matrix product M_z(k).M_y(f).M_x(w), where k, f, w are orientations angles of the camera, i. e., the rotation angles between the image-space and object-space reference systems;
- f is the focal length; and
- a, b are the linear and angular parameters of the image-space straight line, which are extracted by using a feature extraction process.

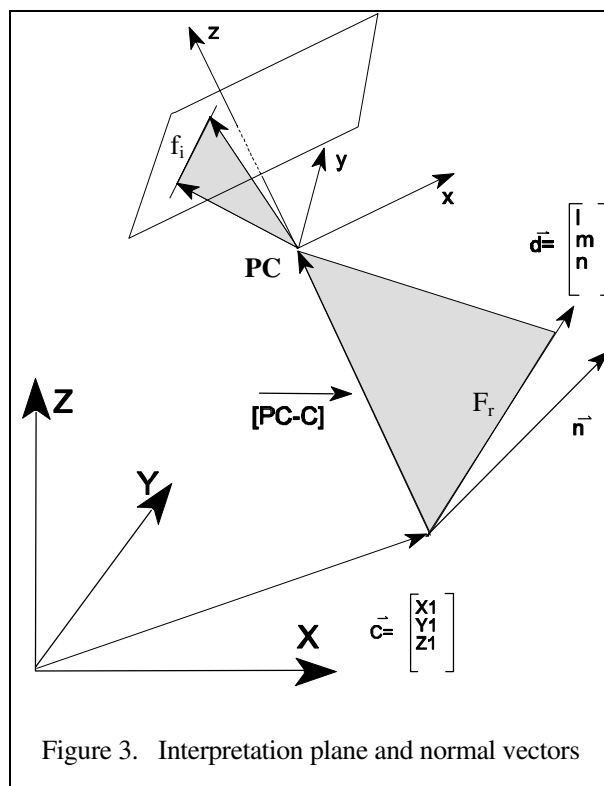


Figure 3. Interpretation plane and normal vectors

However, when the image straight line are close to vertical, the representation y=a.x+b is unstable. In other words, equation 7 can not be used. This problem can be solved using another representation for image straight line, i. e., x=a*.y+b*. Taking into account this representation, the equation 8 can be written:

$$a^* = - \frac{r_{21} \cdot nx + r_{22} \cdot ny + r_{23} \cdot nz}{r_{11} \cdot nx + r_{12} \cdot ny + r_{13} \cdot nz} \tag{8}$$

$$b^* = -f \cdot \frac{r_{31} \cdot nx + r_{32} \cdot ny + r_{33} \cdot nz}{r_{11} \cdot nx + r_{12} \cdot ny + r_{13} \cdot nz}$$

where, all elements were already explained.

The unknowns of photogrammetric model are the exterior orientation parameters (k , f , w , X_o , Y_o , Z_o). These elements are the components of the vector of parameters or the state vector (x_k), which is estimated by an iterative process using equation 9 (Jazwinski, 1970):

$$h_{i+1} = x_{k-1} + k_{k; h_i} \cdot [z_k - h(h_i) - M_{k; h_i} \cdot (x_{k-1} - h_i)] \tag{9}$$

where,

- x_{k-1} is the vector of parameters estimated using a previous correspondence;
- h_i and h_{i+1} are variables for controlling the iterative process and are estimates for x_k in the iterations i and $i+1$, respectively; in the first iteration $h_1 = x_{k-1}$;
- $k_{k; h_i} = P_{k-1} \cdot M_{k; h_i}^T \cdot (M_{k; h_i} \cdot P_{k-1} \cdot M_{k; h_i}^T + R_k)^{-1}$ is the Kalman gain matrix;
- P_{k-1} is the covariance matrix of x_{k-1} ; and
- $M_{k; h_i} = \left. \frac{\partial h(x_k)}{\partial x_k} \right|_{x_k = h_i}$ is the partial derivative matrix computed in the point h_i .

The convergence of the iterative process is reached when $|h_{i+1} - h_i|$ is smaller than a predefined threshold. At this point, the state vector is updated with the last value of the iterative variable h_{i+1} and the state covariance matrix (P_k) is estimated by equation (Jazwinski, 1970):

$$P_k = (I - k_{k; x_k} \cdot M_{k; x_k}) \cdot P_{k-1} \cdot (I - k_{k; x_k} \cdot M_{k; x_k})^T + k_{k; x_k} \cdot R_k \cdot k_{k; x_k}^T \tag{10}$$

where, $M_{k; x_k}$ is computed at the linearization point $x_k = h_{i+1}$ and $k_{k; x_k}$ is computed by using $M_{k; x_k}$.

The predicted residual (v_k) and its covariance matrix (c_k) are computed using equations 11 and 12:

$$v_k = z_k - M_{k; x_k} \cdot x_{k-1} \tag{11}$$

$$c_k = M_{k; x_k} \cdot P_{k-1} \cdot M_{k; x_k}^T + R_k \tag{12}$$

Remembering that the correspondence being analyzed is (f_i , F_i) and that the observations in the filtering are the angular (a or a^*) and linear (b or b^*) parameters of f_i , the data snooping statistical test uses the following values:

$$w_{a/a^*} = \frac{n_{a/a^*}}{S_{a/a^*}} \quad \text{and} \quad w_{b/b^*} = \frac{n_{b/b^*}}{S_{b/b^*}} \tag{13}$$

where,

- n_{a/a^*} is the predicted residual of a or a^* and is the first element of v_k ;

- \hat{n}_{b/b^*} is the predicted residual of b or b^* and is the second element of v_k ;
- S_{a/a^*} is the standard deviation of \hat{n}_{a/a^*} and is the square root of the first element of diagonal of c_k ;
- S_{b/b^*} is the standard deviation of \hat{n}_{b/b^*} and is the square root of the second element of diagonal of c_k ; and
- w_{a/a^*} and w_{b/b^*} are the normalized corrections.

The observations a (or a^*) and b (or b^*) do not have errors when the values w_{a/a^*} and w_{b/b^*} , with the significance level α , are contained in the intervals:

$$-N_{\alpha/2} < w_{a/a^*} < N_{\alpha/2} \quad \text{and} \quad -N_{\alpha/2} < w_{b/b^*} < N_{\alpha/2} \quad (14)$$

where, $N_{\alpha/2}$ is extracted from normal curve.

3 RESULTS WITH REAL DATA

The entire system has been implemented in C language, with a command line user interface and it has been designed to be automatic. All the routines including estimation and image processing were in-house developed.

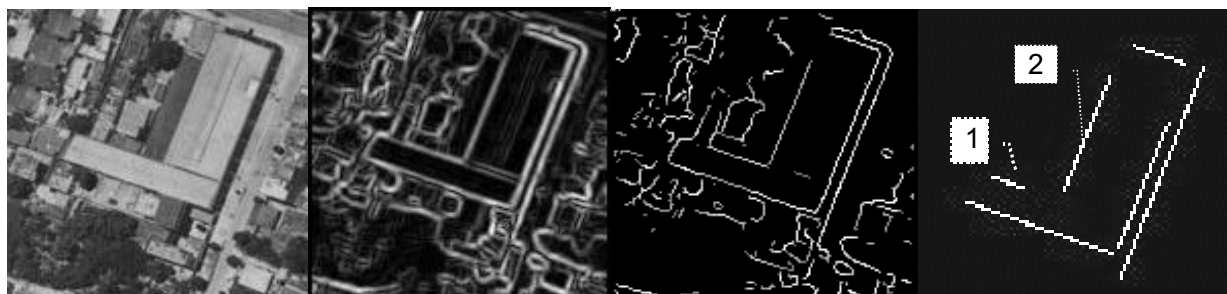


Figure 4. Results from the pipeline for feature extraction and matching

- Window automatically extracted from the original image (grouping 3 – highlighted in table 1);
- Edges obtained by applying the Nevatia and Babu filters and automatic thresholding;
- Thinned edges with non maxima suppression and filtering of isolated elements;
- Straight lines after line fitting. The highlighted lines (1) and (2) were previously known in the object-space and the line (2) was correctly matched.

Experiments with real data were performed in order to verify the potential of the proposed method. A scanned aerial photograph (1:8.000) of Rio de Janeiro City was used. The original image was resampled to a pixel size of $75\mu\text{m}$ in order to facilitate the debugging of the C codes and to avoid a large data set. Experiments with the original data are being conducted and will not be reported in this paper.

Selected Groupings	Number of straight lines	
	Object-space	Image-space
1	4	6
2	6	10
3	2	6
4	2	9
5	2	4
6	2	10

Table 1. Image and object-space groupings

Six grouping of straight lines were selected from building edges using an existing DXF file (1:2000), generated by analytical photogrammetric plotting. Selection of object straight lines was done considering the worst case, i.e., only a few entities for each grouping was collected. In real operation environment much more entities could be selected, improving the final results. The corresponding area of the selected features was automatically searched and the straight lines in the image-space were automatically extracted. Figure 4 shows an example of the feature extraction results and the final results of the matching process for one grouping. Table 1 presents the number of entities both in the image-space and object-space for the selected groupings.

The approximate and refined exterior orientation parameters and their standard deviation are presented in the table 2. Null values were adopted as approximate rotations, with standard deviations of 0.052 rad (3°). On the other hand, the co-ordinates of perspective center were measured by GPS and used as approximate translations. Precision of 30m for X and 10m for Y and Z-axis were assumed. After processing, using the proposed methods, 3 correspondences from grouping 1, 2 from grouping 2, 1 from grouping 3, 1 from grouping 5, and 1 from grouping 6 were obtained. Therefore, the orientation parameters were estimated with 8 correspondences.

	Approximate Values		refined Values	
	Parameter Values	Standard Deviation	Parameter Values	Standard Deviation
κ rad	0	0.052	-0.06988	0.00042
φ rad	0	0.052	-0.00261	0.00235
ω rad	0	0.052	0.02527	0.00341
X_o m	664402	30	664380,9	3,9
Y_o m	7481112	10	7481115,9	5,1
Z_o m	1334	10	1329,0	2,8

Table 2. Approximate and refined exterior orientation parameters and theirs standard deviations

A conventional space resection process using ground control points was performed in order to check the results of the proposed approach. The differences (ϵ) between parameters of a conventional space resection and the proposed approach are presented in table 3. Errors for parameters κ , φ , X_o , and Z_o were greater than the respective standard deviations that are estimated, which was probably caused by small and nearly grouped straight lines, generating weak geometry.

Errors in the exterior orientation parameters					
$\epsilon \kappa$ (rad)	$\epsilon \varphi$ (rad)	$\epsilon \omega$ (rad)	ϵX_o (m)	ϵY_o (m)	ϵZ_o (m)
-0,0111	-0,0051	0,0009	-8,5	2,7	-4,9

Table 3. Errors obtained in the estimation process

Finally, using translation and rotation errors that is obtained in each correspondence, the convergence of IEKF in the matching process is presented in the figure 5.

The following conclusions can be derived from this figure:

- The selected groupings were not good enough to provide a high precision solution;
- IEKF starts to converge after the second correspondence, except in κ . This can be explained by the weak geometry provided by a few and small straight lines; and
- Even with this weak geometry all the correspondences were correctly established and the filter converged properly.

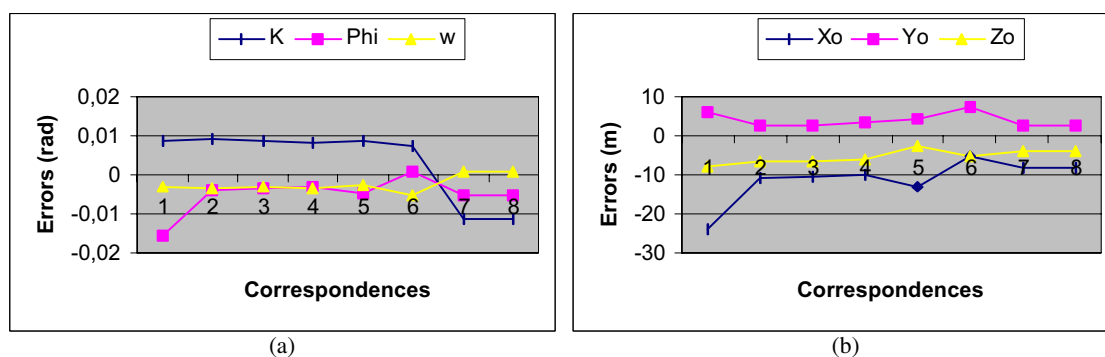


Figure 5. Convergence of the IEKF. (a) Rotations; and (b) Translations.

4 CONCLUSIONS

A line based method aiming automatic orientation of digital aerial images has been proposed and tested. This method is based on automatic feature extraction techniques, relational matching and a mathematical model specifically derived to work with straight lines.

Experiments performed with real data have demonstrated the potential of the proposed solution. More empirical investigations are being conducted in order to assess the optimal configuration of straight lines to provide high quality results.

ACKNOWLEDGEMENTS

This work was supported by FAPESP (*Fundação de Amparo à Pesquisa do Estado de São Paulo*) and CNPQ (*Conselho Nacional de Pesquisa e Desenvolvimento*). The scanned aerial photograph and the DXF files used in our experiments have been kindly provided by Esteio - Engenharia e Aerolevantamentos Ltda.

REFERENCES

- Ballard, D.H. and Brown, C.M. , 1982. *Computer Vision*, New Jersey: Prentice-Hall. 522p.
- Burns, J.B.; Hanson, A. B.; Riseman, E. M., 1986. Extracting straight lines, *IEEE Transactions on PAMI* 8, pp. 425-455.
- Dal Poz, A.P.; Tommaselli, A.M.G.; Cintra, J.P., 1996. Relational Matching Applied to Automatic Extraction of Ground Control in Digital Images. In: *International Archives of Photogrammetry and Remote Sensing*, Vienna, Austria, pp. 131-134.
- Dal Poz, A.P.; Tommaselli, A.M.G. 1998 Strategy to detect ground control in digital images. In: *Automatic Target Recognition 8. Proceedings of the SPIE*, Orlando, Fl, EUA, Vol. 3371, pp. 436-447.
- Dhome, M.; Richetin, M.; Lapresté, J. And Rives, G., 1989. Determination of the attitude of 3-D objects from a single perspective view, *IEEE Transactions on PAMI*, 11(12), pp. 1265-1278.
- Dowman, I.J.; Morgado, A.; Vohra, V., 1996. Automatic Registration of images with maps using polygonal features. In: *International Archives of Photogrammetry and Remote Sensing*, Vienna, Austria, pp. 139-145.
- Jazwinski, A. H., 1970. *Stochastic Processes and Filtering Theory*, Academic Press, INC..
- Mulawa, D. C.; Mikhail, E. M., 1988. Photogrammetric treatment of linear features. In: *International Archives of Photogrammetry and Remote Sensing*, 1988, Kyoto, pp. 383-393.
- Shapiro, L. G.; Haralick, R. M., 1987. Relational Matching. *Applied Optics*, 26, pp. 1845-1851.
- Sonka, M.; Hlavac, V.; Boyle, R., 1993 *Image Processing, Analysis and Machine Vision*. Chapman & Hall, London, 555p.
- Tommaselli, A.M.G.; Lugnani, J. B., 1988. An alternative mathematical model to the collinearity equation using straight features. In: *International Archives of Photogrammetry and Remote Sensing*, Kyoto, pp. 765-774.
- Tommaselli, A.M.G.; Tozzi, C. L., 1996. A recursive approach to Space Resection using straight lines. *Photogrammetric Engineering and Remote Sensing*. 62(1), pp. 57-66.
- Tommaselli, A. P. ; Dal Poz, A. P., 1999. Line based orientation of aerial images. Automatic Extraction of GIS Objects from Digital Imagery, ISPRS Conference by ISPRS Working Groups II/6, II/8, III/1, III/2, III/3, III/4, Munique, 6-10 Sep.